Oscillations and Coupling in Interconnections of Two-Dimensional Brain Networks

Erfan Nozari Jorge Cortés

Abstract— **Oscillations in the brain are one of the most ubiquitous and robust patterns of activity and correlate with various cognitive phenomena. In this work, we study the existence and properties of oscillations in simple mean-field models of brain activity with bounded linear-threshold rate dynamics. First, we obtain exact conditions for the existence of limit cycles in two-dimensional excitatory-inhibitory networks (E-I pairs). Building on this result, we study networks of multiple E-I pairs, provide exact conditions for the lack of stable equilibria, and numerically show that this is a tight proxy for the existence of oscillatory behavior. Finally, we study cross-frequency coupling between pairs of oscillators each consisting of an E-I pair. We find that while both phase-phase coupling (synchronization) and phase-amplitude coupling (PAC) monotonically increase with inter-oscillator connection strength, there exists a tradeoff in increasing frequency mismatch between the oscillators as it desynchronizes them while enhancing their PAC.**

I. Introduction

Since Berger's groundbreaking discovery of oscillatory activity in the brain [1], oscillations have been found in a wide range of species and brain regions and multiple studies have shown the correlation between their properties (amplitude, phase, shape, coupling, etc.) and various neurocognitive processes. Despite their importance, our understanding of brain oscillations is far from complete. Here, we take an analytical approach and study network models with linear-threshold rate dynamics, revealing the relationship between network structure and oscillatory behavior, both within a single region and when coupled between multiple regions.

Literature review: Oscillations have been the subject of extensive research in the neuroscience literature, see, e.g. [2], [3]. In addition to the vast number of experimental and computational works, several efforts have pursued analytical model-based approaches, particularly using mean-field models such as the Wilson-Cowan model [4]. However, the sigmoidal nonlinearity in the Wilson-Cowan model has not allowed more than partial characterizations [5]–[8] of structural conditions giving rise to oscillations. Motivated by this, [9] studies oscillations and synchronization in Wilson-Cowan models with bounded linear-threshold nonlinearities, but relies on unrealistic assumptions (excluding interaction terms in the nonlinearities, having mixed excitatory-inhibitory nodes (i.e., violating Dale's law), and a chain network topology) to obtain rigorous results. Linear-threshold networks are indeed capable of modeling a wide range of (nonlinear) phenomena such as mono-, bi-, and multi-stability, limit cycles, and chaos [10]. While the existence and uniqueness of equilibria and asymptotic stability are reasonably well understood, see [11] and references therein, our understanding of their oscillatory behavior has remained limited.

A growing body of research has also studied brain oscillations using models of phase oscillators such as the Kuramoto model, see [12]–[14] and references therein. This is motivated by the fact [15] that the Kuramoto model is a local approximation to the Wilson-Cowan model (around zero interconnection strength) and has the advantage of having smaller state dimensions. Nevertheless, this also comes at the expense of different global behaviors (when coupling is large), cf. [16], and the exclusion of amplitude dynamics that are essential to neuronal phenomena such as PAC.

Statement of contributions: Our contributions are threefold. First, we obtain an exact characterization of existence of limit cycles for two-dimensional excitatory-inhibitory network motifs described by bounded linear-threshold dynamics (*E-I pairs*). These two-dimensional motifs serve as models of small brain regions that can then be connected to model large-scale brain dynamics. Accordingly, our second contribution is the study of such networks of oscillators with arbitrary size and connectivity where each oscillator is itself an E-I pair. We derive exact conditions for the lack of stable equilibria and show, through extensive simulations, that this condition is indeed a tight proxy for oscillatory behavior. Finally, using this condition, we study synchronization and PAC as the two most prominent forms of oscillatory coupling in the brain. We show numerically that increasing the inter-oscillator connectivity strength has the same (enhancing) effect on both synchronization and PAC, while increasing frequency mismatch between the oscillators has an opposing effect on them (decreasing synchronization, increasing PAC). Together, these analytical and numerical results provide great insight into the nature of brain oscillations and its relation to the structure of the underlying networks. For space reasons, all proofs are omitted and will appear elsewhere.

Notation: We let $\mathbb{R}$, $\mathbb{R}_{>0}$, and $\mathbb{R}_{\geq 0}$ denote the set of reals, positive reals, and nonnegative reals, resp. For $a, b \in \mathbb{R}$, $\mathcal{U}(a,b)$ denotes the uniform distribution over $[a,b]$. We use bold-faced letters for vectors and matrices. $\mathbf{1}_n$ and $\mathbf{I}_n$ stand for the n-vector of all ones and the identity n-by-n matrix, and we omit subscripts when clear from the context. Given a vector $\mathbf{x}$, x_i and $(\mathbf{x})_i$ refer to its ith component and, if block-partitioned, $\mathbf{x}_i$ refers to its ith block. Likewise, A_{ij} refers to the (i,j)th entry of matrix $\mathbf{A}$. Given $\mathbf{m} \in \mathbb{R}^n_{>0}$, $[\mathbf{0}, \mathbf{m}] = [0, m_1] \times \cdots \times [0, m_n]$. For $x \in \mathbb{R}$, $[x]_0^m = \min\{\max\{x, 0\}, m\}$, which is extended entry-wise to $[\mathbf{x}]_{\mathbf{0}}^{\mathbf{m}}$.

This work was supported by NSF Award CMMI-1826065 (EN and JC) and ARO Award W911NF-18-1-0213 (JC).

E. Nozari and J. Cortés are with the Department of Mechanical and Aerospace Engineering, UC San Diego, {enozari,cortes}@ucsd.edu.

II. Problem Formulation

Consider a neuronal network composed of a large number of neurons that communicate with each other via asynchronous sequences of spikes. Grouping together neurons with similar firing rates, under standard assumptions[1], the mean-field dynamics of the network can be described by the linear-threshold model

$$\tau\dot{\mathbf{x}}(t) = -\mathbf{x}(t) + [\mathbf{W}\mathbf{x}(t) + \mathbf{u}]_{\mathbf{0}}^{\mathbf{m}}, \qquad \mathbf{x}(0) \in [\mathbf{0}, \mathbf{m}], \quad (1)$$

where $\mathbf{x} \in \mathbb{R}^N_{\geq 0}$ is the state vector with components x_i denoting the average firing rate of the i'th neuronal population, $i \in \{1, \dots, N\}$, $\mathbf{W} \in \mathbb{R}^{N\times N}$ is the matrix of average synaptic connectivities, $\mathbf{u} \in \mathbb{R}^N$ is the vector of average external (background) inputs to the populations, $\mathbf{m} \in \mathbb{R}^N_{>0}$ is the vector of average maximum firing rates, and $\tau > 0$ is the network time constant. Note that $[\mathbf{0}, \mathbf{m}]$ is invariant under (1), ensuring, in particular, that all solutions are bounded.

Our previous work [11] has characterized the existence and uniqueness of equilibria and asymptotic stability for a variant of (1) with an unbounded activation function ($\mathbf{m} = \infty \cdot \mathbf{1}_N$), and these results are readily extensible to arbitrary finite $\mathbf{m}$. However, the existence of oscillations in linear-threshold dynamics is not as well understood. Further, brain networks often contain interconnections of multiple coupled oscillators, but our understanding is even slimmer about the oscillatory behavior of interconnections of linear-threshold networks of the form (1).

Our goal is to characterize the relationship between network structure and the oscillatory behavior observed in linear-threshold dynamics modeling brain networks. We formalize the problem of interest as follows.

Problem 1. *For the bounded linear-threshold network dynamics* (1)*, characterize the relationship between network structure* $(\mathbf{W}, \mathbf{m}, \mathbf{u})$ *and*

(i) existence of oscillations in a single network (1)*;*
(ii) existence/preservation of oscillations in a network of oscillatory networks, each modeled by (1)*;*
(iii) phase-phase coupling (synchronization) and phase-amplitude coupling (PAC) between pairs of oscillators.

Questions (i) and (ii) arise naturally as the first steps towards understanding oscillatory behavior of (1). On the other hand, synchronization (i.e., the phase-locking of two oscillators with the same frequency) and PAC (i.e., the dependence of the amplitude of a high-frequency oscillator on the phase of a low-frequency one), are of specific interest as they are the most widely observed and studied oscillatory coupling phenomena in brain networks. Examples of these phenomena are shown in Figure 1. We address (i) and (ii) in Section III and (iii) in Section IV.

Following common practice in computational neuroscience, we here adopt a broad notion of oscillations that includes both periodic oscillations (limit cycles) and chaotic ones. In the latter case, a chaotic behavior is oscillatory if its state trajectories are near-periodic or, equivalently, have power spectra with distinct and pronounced resonance peaks.

[1]See, e.g., [17, Ch 7] for a comprehensive exposition or [11] for a brief discussion.

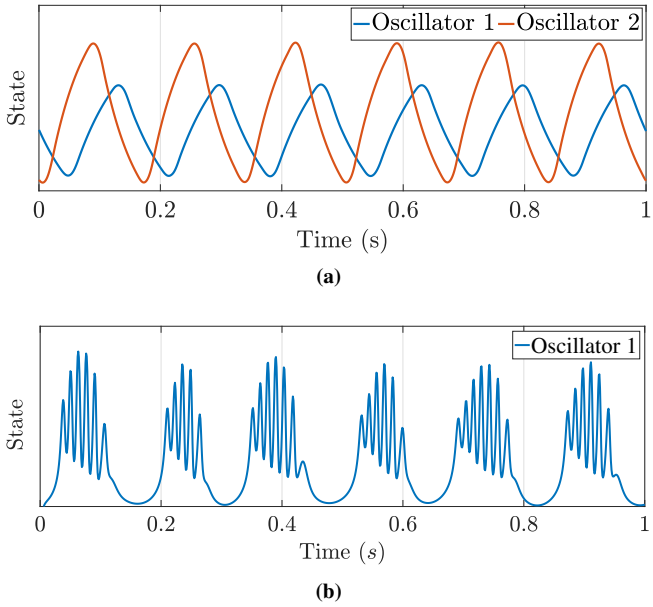

Fig. 1: Examples of (a) synchronization and (b) PAC in models of neuronal activity. Note that while both phenomena occur as a result of the interaction of two oscillators, synchronization is defined (and measured) between the trajectories of both oscillators but PAC is defined (and measured) between two frequency components of each trajectory.

III. Existence of Oscillations

In this section we analyze the dynamics (1) and derive conditions on the network structure $(\mathbf{W}, \mathbf{m}, \mathbf{u})$ giving rise to oscillatory behavior. The analytical tools in the study of oscillations are generally limited to 2-dimensional systems (cf. the Poincaré-Bendixson theory [18, Ch 3]) or higher-dimensional systems that are essentially confined to 2-dimensional manifolds (see, e.g., [19], [20]). Thus, we start our analysis by 2-dimensional networks and then extend the results to arbitrarily large interconnections of 2-dimensional oscillators.

A. Two-Dimensional Excitatory-Inhibitory Oscillators

An important property of biological neuronal networks, known as Dale's law [4], [17], is that each node has either an excitatory (E) or inhibitory (I) effect on other nodes, but not both. This means that each column of $\mathbf{W}$ is either nonnegative or nonpositive. Thus, a 2-dimensional network can be either E-E, I-I, or E-I. The latter, hereafter called an *E-I pair*, is also known as the Wilson-Cowan model and has been widely used in computational neuroscience for decades [4]–[8]. Unlike the standard Wilson-Cowan model that uses sigmoidal activation functions, we show in the following that a complete characterization of limit cycles can be obtained for E-I pairs with bounded linear-threshold nonlinearities.

According to the Poincaré-Bendixson theory [18, Ch 3], in a two-dimensional system ($N = 2$), the lack of stable

equilibria is, under mild conditions, necessary and sufficient for the existence of almost globally (excluding trajectories starting at an unstable equilibrium) asymptotically stable limit cycles. To study the equilibria of (1), we use its representation as a switched affine system. It is straightforward to show [11] that $\mathbb{R}^N$ can be decomposed into 3^N switching regions $\{\Omega_{\boldsymbol{\sigma}}\}_{\boldsymbol{\sigma}\in\{0,\ell,\mathrm{s}\}^N}$ defined by

$$\begin{aligned}\Omega_{\boldsymbol{\sigma}} = \{\mathbf{x} \mid\ & (\mathbf{W}\mathbf{x}+\mathbf{u})_i \in (-\infty, 0], \quad \forall i \ \text{ s.t. } \ \sigma_i = 0, \text{ and} \\ & (\mathbf{W}\mathbf{x}+\mathbf{u})_i \in [0, m_i], \quad \forall i \ \text{ s.t. } \ \sigma_i = \ell, \text{ and} \\ & (\mathbf{W}\mathbf{x}+\mathbf{u})_i \in [m_i, \infty), \quad \forall i \ \text{ s.t. } \ \sigma_i = \mathrm{s}\},\end{aligned}$$

where 0, ℓ, and s denote inactive, active (linear), and saturated nodes, respectively. Thus, (1) can be rewritten in the switched affine form

$$\tau\dot{\mathbf{x}} = (-\mathbf{I} + \boldsymbol{\Sigma}^{\ell}\mathbf{W})\mathbf{x} + \boldsymbol{\Sigma}^{\ell}\mathbf{u} + \boldsymbol{\Sigma}^{\mathrm{s}}\mathbf{m}, \qquad \forall \mathbf{x} \in \Omega_{\boldsymbol{\sigma}}, \quad (2)$$

where for any $\boldsymbol{\sigma} \in \{0, \ell, \mathrm{s}\}^N$, $\boldsymbol{\Sigma}^{\ell} \in \mathbb{R}^{N\times N}$ is a diagonal matrix with diagonal entries

$$\Sigma^{\ell}_{ii} = \begin{cases} 1 & \text{if} \quad \sigma_i = \ell, \\ 0 & \text{if} \quad \sigma_i = 0, \mathrm{s}, \end{cases}$$

and, likewise, $\boldsymbol{\Sigma}^{\mathrm{s}} \in \mathbb{R}^{N\times N}$ is a diagonal matrix with diagonal entries

$$\Sigma^{\mathrm{s}}_{ii} = \begin{cases} 1 & \text{if} \quad \sigma_i = \mathrm{s}, \\ 0 & \text{if} \quad \sigma_i = 0, \ell. \end{cases}$$

Each $\Omega_{\boldsymbol{\sigma}}$ then has a corresponding *equilibrium candidate*

$$\mathbf{x}^*_{\boldsymbol{\sigma}} = (\mathbf{I} - \boldsymbol{\Sigma}^{\ell}\mathbf{W})^{-1}(\boldsymbol{\Sigma}^{\ell}\mathbf{u} + \boldsymbol{\Sigma}^{\mathrm{s}}\mathbf{m}),$$

and the equilibria of (1) consist of all $\mathbf{x}^*_{\boldsymbol{\sigma}}$ that belong to their respective switching regions. This allows us to derive an exact characterization of limit cycles for E-I pairs, as stated next.

Theorem III.1. ***(Limit cycles in E-I pairs).*** *Consider the dynamics* (1) *with* $N = 2$ *and*

$$\mathbf{W} = \begin{bmatrix} a & -b \\ c & -d \end{bmatrix}, \qquad a, b, c, d \geq 0.$$

All network trajectories (except those starting at an unstable equilibrium, if any) converge to a limit cycle if and only if

$$d + 2 < a, \quad (3a)$$

$$(a-1)(d+1) < bc, \quad (3b)$$

$$(a-1)m_1 < bm_2, \quad (3c)$$

$$0 < u_1 < bm_2 - (a-1)m_1, \quad (3d)$$

$$0 < (d+1)u_1 - bu_2 < \big[bc - (a-1)(d+1)\big]m_1. \quad (3e)$$

The conditions of Theorem III.1 have simple biological intuitions. Equation (3a) requires the positive feedback among the neurons of the excitatory population[2] to be sufficiently stronger than the negative feedback among the inhibitory population. This, together with the strong mutual coupling (3b) between the two populations, ensures local instability of the equilibrium point $\mathbf{x}^*_{(\ell,\ell)}$ and prevents the oscillations from damping. On the other hand, condition (3c) ensures that the *upper bound* on the inhibitory input to the excitatory population (bm_2) is high enough to balance the strong self-excitation. This is consistent with thin spike widths and high firing rates of the inhibitory "fast-spiking interneurons" in the cortex and the theory of excitatory-inhibitory (E-I) balance [21]. Finally, the conditions (3d) and (3e) require that the external inputs to the two nodes are neither excessively low nor excessively high, as it would keep the respective nodes in negative or positive saturation, resp., which would reduce the effective dimensionality of the network to less than two and make oscillations impossible. We build on this result next to study the oscillatory behavior of a network of oscillators, each represented by an E-I pair.

[2]Recall that each node of the network dynamics (1) represents one population of neurons with similar activity patterns.

B. Networks of Two-Dimensional Oscillators

Consider n oscillators, each modeled by an E-I pair, connected over a network with adjacency matrix $\mathbf{A} \in \mathbb{R}^{n\times n}_{\geq 0}$ via their excitatory nodes [22]. Since $\mathbf{A}$ captures inter-oscillator connections, its diagonal entries are zero. Thus, the dynamics of the resulting network of networks is

$$\mathbf{T}\dot{\mathbf{x}} = -\mathbf{x} + [\mathbf{W}\mathbf{x} + \mathbf{u}]^{\mathbf{m}}_{\mathbf{0}}, \quad (4a)$$

where

$$\mathbf{x} = \begin{bmatrix} \mathbf{x}_1^T & \cdots & \mathbf{x}_n^T \end{bmatrix}^T, \quad \mathbf{x}_i = \begin{bmatrix} x_{i,1} \\ x_{i,2} \end{bmatrix}, \quad (4b)$$

$$\mathbf{T} = \mathrm{diag}(\tau_1, \tau_1, \tau_2, \tau_2, \ldots, \tau_n, \tau_n), \quad (4c)$$

$$\mathbf{W} = \mathrm{diag}(\mathbf{W}_1, \ldots, \mathbf{W}_n) + \mathbf{A} \otimes \mathbf{E}, \ \mathbf{E} = \begin{bmatrix} 1 & 0 \\ 0 & 0 \end{bmatrix}, \quad (4d)$$

$$\mathbf{W}_i = \begin{bmatrix} a_i & -b_i \\ c_i & -d_i \end{bmatrix}, \quad A_{ii} = 0, \quad i \in \{1, \ldots, n\}, \quad (4e)$$

$\mathbf{u}$ and $\mathbf{m}$ have similar decompositions to $\mathbf{x}$, and $\otimes$ denotes the Kronecker product.

We consider the case where each E-I pair oscillates on its own. The first question we address is whether the pairs maintain any oscillatory behavior after their interconnection. Since conditions for the existence of limit cycles in systems with higher than two dimensions are in general unknown, we use the lack of stable equilibria (which constitutes the main condition in the Poincaré-Bendixson theory for existence of limit cycles) as a proxy for oscillations. Later in Section III-B, we show numerically that this proxy is indeed a tight characterization of oscillatory dynamics.

Theorem III.2. ***(Lack of stable equilibria in networks of E-I pairs).*** *Consider the dynamics* (4) *and assume that each* $\mathbf{W}_i$ *satisfies the conditions of Theorem III.1. Then, the overall network does not have any stable equilibria if and only if*

$$\sum_{j=1}^{n} A_{ij} m_{j,1} < \bar{u}_{i,1} - u_{i,1}, \quad (5)$$

$$\bar{u}_{i,1} \triangleq b_i \min\left\{m_{i,2}, \frac{u_{i,2} + c_i m_{i,1}}{d_i + 1}\right\} - (a_i - 1)m_{i,1},$$

holds for at least one $i \in \{1,\dots,n\}$. Moreover, the state of any E-I pair for which (5) *holds may not converge to a fixed value (except for trivial solutions starting at unstable equilibria, if any) irrespective of the validity of* (5) *for other pairs.*

Theorem III.2 provides a precise characterization of the lack of stable equilibria for the network dynamics (4). Even though the lack of stable equilibria is in principle neither necessary nor sufficient for the existence of limit cycles, we show next that it is in fact almost necessary and sufficient for the existence of oscillatory behavior. Nevertheless, such oscillatory behavior is often chaotic, not a limit cycle, which may have more relevance for neuronal oscillations [23].

IV. Oscillatory Properties and Coupling

In this section, we focus on the properties of oscillations generated by (4) under the conditions of Theorem III.2. First, we show that the lack of stable equilibria (and thus (5)) is indeed a tight proxy for existence of oscillations. Then, motivated by the experimental and computational evidence in brain networks, we study the phenomena of synchronization and phase-amplitude coupling.

A. Regularity of Oscillations

To assess the oscillatory behavior of the networks that satisfy (5), we construct random networks according to

$$\begin{aligned} &d_i \sim \mathcal{U}(0, d_{\max}), \quad a_i \sim \mathcal{U}(a_{\min}, a_{\max}),\ a_{\min} > d_{\max} + 2,\\ &b_i = c_i \sim \mathcal{U}(b_{\min}, b_{\max}),\ b_{\min} > \sqrt{(a_{\max}-1)(d_{\max}+1)},\\ &m_{j,i} \sim \mathcal{U}(m_{j,\min}, m_{j,\max}),\ m_{2,\min} > \frac{a_{\max}-1}{b_{\min}} m_{1,\max},\\ &\tau_i \sim \mathcal{U}(\tau_{\min}, \tau_{\max}), \quad \text{i.i.d. } \forall j = 1,2, i \in \{1,\dots,n\}, \end{aligned} \tag{6}$$

all satisfying (3a)-(3c). The values of $u_{i,1}$ and $u_{i,2}$ are always chosen at the center of their respective ranges in (3d)-(3e) in order for the E-I pairs to oscillate at their maximum amplitude before interconnection. For $\mathbf{A}$, we first generate a random $\mathbf{G} \in \mathbb{R}^{n\times n}_{\geq 0}$ with zero diagonal and i.i.d. $\mathcal{U}(0,1)$-distributed off-diagonal entries and set

$$\mathbf{A} = \eta \bar{\mathbf{A}}, \quad \bar{\mathbf{A}} = \operatorname{diag}(\bar{\mathbf{u}}_1 - \mathbf{u}_1)\mathbf{G}[\operatorname{diag}(\mathbf{G}\mathbf{1}_n)\operatorname{diag}(\mathbf{m}_1)]^{-1}.$$

$\mathbf{A}$ then satisfies (5) for all $i \in \{1,\dots,n\}$ if and only if $\eta \in [0,1)$.

To measure the existence of oscillations, we use the notion of regularity of oscillations. Given a *zero-mean* signal $x(t)$, we construct a *regularity index* as follows. Let $X(f)$ be the Fourier transform of $x(t)$, $f_{\max} = \arg\max_f |X(f)|$, and

$$\chi_{\text{reg}} = \frac{|X(f_{\max})|}{\max\{|X((1-\epsilon)f_{\max})|, |X((1+\epsilon)f_{\max})|\}} \in [1,\infty),$$

where $\epsilon \in (0,1)$. $\chi_{\text{reg}} = 1$ indicates a flat power spectrum (lack of oscillations) whereas $\chi_{\text{reg}} \to \infty$ indicates a Dirac delta at $f_{\max}$ (perfectly regular oscillations). In practice, values of $\chi_{\text{reg}} \gtrsim 2$ for $\epsilon \lesssim 0.1$ capture oscillatory behavior, with more regularity (less chaotic behavior) as χ_{reg} grows.

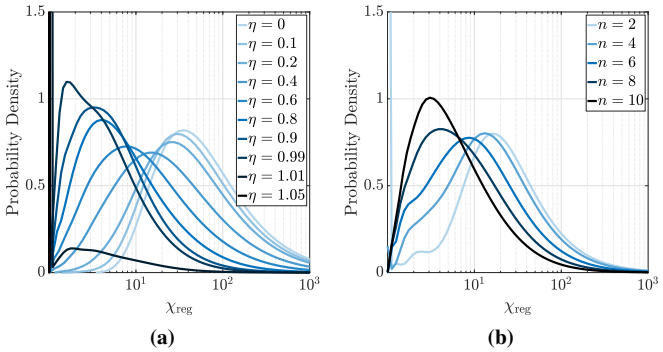

(a) **(b)**

Fig. 2: Regularity of oscillations as a function of network size (n) and inter-oscillator connection strength (η). The probability density function of $\log \chi_{\text{reg}}$ is plotted for **(a)** $n = 10$ and varying η and **(b)** $\eta = 0.9$ and varying n. Each distribution is based on 500 random networks (6) with $d_{\max} = 1$, $a_{\min} = 3.5$, $a_{\max} = 5$, $b_{\min} = \sqrt{8} + 0.5$, $b_{\max} = \sqrt{8} + 2$, $m_{1,\min} = 1$, $m_{1,\max} = 2$, $m_{2,\min} = 8/b_{\min} + 0.5$, $m_{2,\max} = 8/b_{\min} + 2$, $\tau_{\min} = 1$, $\tau_{\max} = 10$.

Figure 2(a) shows the probability distribution of χ_{reg} for random networks of $n = 10$ oscillators ($N = 20$ nodes), $\epsilon = 0.1$, and varying interconnection strength η. For disconnected oscillators ($\eta = 0$), each oscillator has a perfectly regular oscillation (by Theorem III.1) and thus very large χ_{reg} (though finite due to finite signal length and numerical error). These oscillations lose their regularity as we increase the connection strength η towards 1, but still persist up to $\eta = 0.99$, showing the almost sufficiency of (5). Further, moving beyond $\eta = 1$, about 10% of oscillations persist at $\eta = 1.01$ but all disappear at $\eta = 1.05$ due to convergence to the stable equilibria ensured by Theorem III.2. This shows that (5) is also almost necessary for existence of oscillations in the network dynamics (4).

In addition to η, the regularity of oscillations also depend on the network size. Figure 2(b) shows the distribution of χ_{reg} for networks of varying size at $\eta = 0.9$. Interestingly, network oscillations lose regularity as we increase network size, which is in line with existing observations on the relation between chaos and network size [24].

Figure 2 suggests, indirectly via the regularity of oscillations, that the network dynamics (4) become increasingly chaotic as either n or η increases. To assess this more directly, we compute the maximal Lyapunov exponent (MLE) for random networks with the same statistics as (6), cf. Figure 3. MLE measures the exponential rate at which the norm of the solutions of the linearization of the dynamics around a certain trajectory (network attractor in this case) grow or decay. Therefore, a positive MLE is traditionally used as an indication of chaos [25]. As expected, Figure 3 shows a clear increase in MLE both as a function of $\eta < 1$ and n, while moving η beyond 1 rapidly decreases MLE.

Somewhat surprisingly, even though at $\eta = 0$ each E-I pair has a perfectly regular oscillation (limit cycle) giving an individual MLE of 0 (see also [26], [27]), the network dynamics (4) is still slightly chaotic, potentially due to the mismatch between the periods of the individual oscillators.

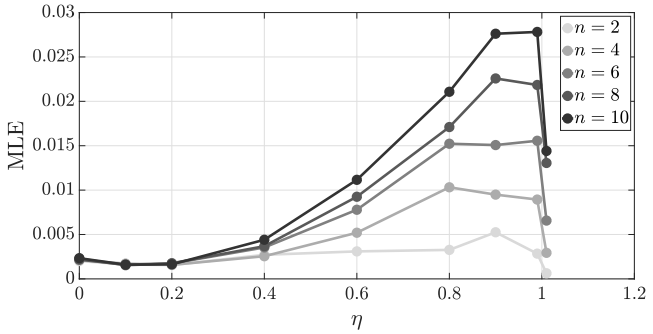

Fig. 3: Maximal Lyapunov exponent for varying network size n and inter-oscillator connection strength η. Each point is the average MLE of 200 networks with the same statistics as in Figure 2.

Interestingly, increasing η up to ~ 0.2 *enhances* order among the oscillators due to their effort to synchronize. This further motivates the analysis of synchronization within the network (cf. Problem 1(iii)), which we tackle next.

B. Synchronization and Phase-Amplitude Coupling

The literature is rich in measures of synchronization, see e.g., [28] for a review and comparison of different methods. Given two discrete signals $z_1(k), z_2(k), k \in \{1, \dots, K\}$, we use the measure of phase synchronization

$$\chi_{\text{sync}} = \left| \frac{1}{K} \sum_{k=1}^{K} e^{j(\phi_1(k) - \phi_2(k))} \right| \in [0, 1], \tag{7}$$

where $\phi_i(k)$ is the instantaneous phase[3] of $\{z_i(k)\}_{k=1}^K$. This is simply a circular average of the phase difference between the two oscillators, giving a value of 1 if the two oscillators are phase-locked and about 0 if they oscillate independently.[4]

Figure 4(a) shows the average value of χ_{sync} as a function of interconnection strength η for pairs of oscillators ($n = 2, N = 4$) with the same statistic as in (6), except that the values of the time constants τ_1 and τ_2 are chosen precisely to obtain a desired ratio ω_1/ω_2 of their natural frequencies. Similar to networks of phase oscillators such as the Kuramoto model [12], networks with $\omega_1 = \omega_2$ are always synchronized irrespective of η, while synchronization increases with η and decreases with frequency mismatch ω_1/ω_2. However, the important distinction with the Kuramoto model is that here it is not possible to fully synchronize arbitrary pairs of oscillators by increasing their connection strength since oscillations vanish for $\eta > 1$ (the so-called *oscillator death* due to saturation [16]). This results in a more realistic synchronization scheme and is consistent with the fact [15] that the Kuramoto model approximates E-I dynamics similar to (3) only locally around $\eta = 0$ (a.k.a. weakly coupled oscillators).

Next, we move to the analysis of PAC as given in Problem 1(iii). Here, we study the same random networks of

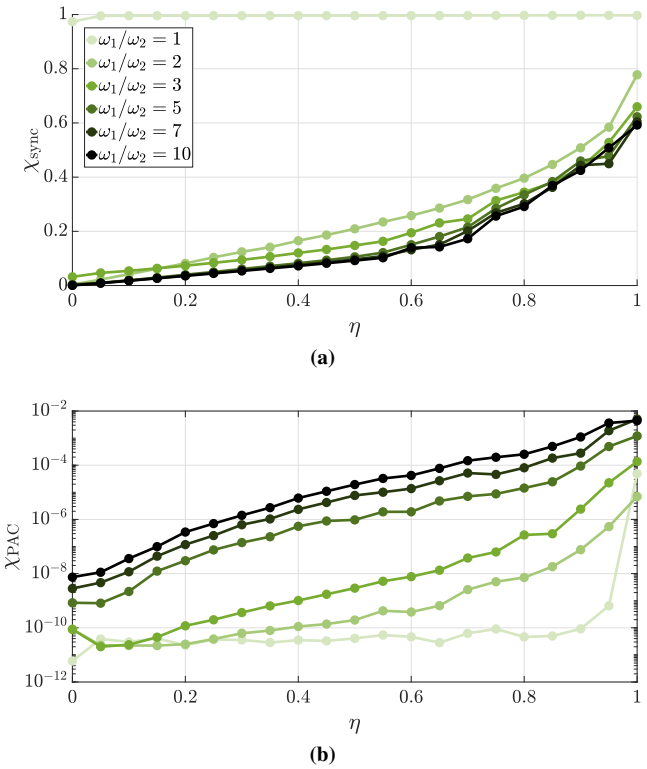

Fig. 4: Cross-frequency coupling between pairs of oscillators. The average value of **(a)** χ_{sync} and **(b)** χ_{PAC} is plotted for pairs of oscillators with varying ratios of natural frequencies ω_1/ω_2 and connection strength η and the same statistics as in Figure 2.

$n = 2$ oscillators as above and see how strongly the phase of the slower oscillator affects the frequency of the faster one. To measure PAC in any signal[5] $\{z(k)\}_{k=1}^K$, we use the measure

$$\chi_{\text{PAC}} = \frac{D_{\text{KL}}(P_A \parallel \mathcal{U}(-\pi, \pi))}{\log(N_{\text{bin}})} \in [0, 1],$$

recommended in [30] following a comparison of several measures available in the literature. Here, we first bandpass-filter z around the two frequency ranges of interest to obtain a slow component z_{slow} and a fast one z_{fast}. Then, we bin the instantaneous phases of z_{slow} into N_{bin} bins and for each bin, compute the average instantaneous amplitude of z_{fast} over that bin.[6] This gives a phase distribution P_A over $[-\pi, \pi]$ that is uniform in the absence of PAC but is centered around a "preferred phase" if the amplitude of z_{fast} is larger at a certain phase of z_{slow}. The measure χ_{PAC} then computes the KL divergence of P_A from the uniform distribution, normalized by its maximum possible value.[7]

Figure 4(b) shows the value of χ_{PAC} for the same networks as in Figure 4(a). Interestingly, χ_{PAC} also increases

[3]We here use Hilbert transform to obtain the instantaneous phase. For a review and comparison of different methods, see [29].

[4]To avoid edge effects and initial transients, we always compute (7) over a middle portion of $\{\phi_i(k)\}_{k=1}^K, i = 1, 2$, for K equal to 10^3 times the period of the slower oscillator.

[5]Note that unlike synchronization, PAC is defined and measured for a single signal, even though it arises as a result of the interaction between two oscillators. Throughout, we measure PAC using the state of the excitatory node of the faster oscillator.

[6]We compute both the instantaneous phases and amplitudes using the Hilbert transform and use $N_{\text{bin}} = 10$ throughout.

[7]As a reference, $\chi_{\text{PAC}} \sim 10^{-4}$ for θ-γ coupling in rodents hippocampus [30] (being a prominent example of PAC in neural data).

as a function of η, similarly to χ_{sync} but it *increases* as a function of frequency mismatch between the oscillators. This shows, for the first time, a clear trade-off between synchronization and PAC, with χ_{PAC} reaching in vivo values of $\sim 10^{-4}$ only for large values of frequency mismatch $\omega_1/\omega_2 \gtrsim 5$ and strong coupling $\eta \gtrsim 0.7$. Note that this tradeoff (and PAC in general) cannot be observed or explained using models of phase oscillators that exclude amplitude dynamics, such as Kuramoto. These results also match observations in the brain, where the most prominent examples of PAC are between theta (4-8$^{\text{Hz}}$) and gamma (30-100$^{\text{Hz}}$) frequency ranges with $\omega_1/\omega_2 \gtrsim 5$ [30], providing an exciting and promising encouragement for further analysis and understanding of the structure of the underlying brain networks.

V. Conclusions and Future Work

We have studied the existence of oscillations and cross-frequency coupling in brain networks with bounded linear threshold rate dynamics. We have provided a complete characterization of structural parameters in two-dimensional E-I pairs that generate limit cycles as well as generalizations to higher dimensional networks of E-I pairs. We further showed that this class of models can generate synchronization and PAC similar to in vivo observations and that both phenomena increase with inter-oscillator connection strength while having an opposite dependence on inter-oscillator frequency mismatch. Future work will include the generalization of our results to arbitrary network structures with higher than two dimensions, analytical characterization of the effects of inter-oscillator connectivity strength and frequency mismatch on synchronization and PAC, exploring the applications of these results to in vivo recordings and information transfer, and generalizations to incorporate conduction delays and noise.

References

[1] H. Berger, "Über das elektrenkephalogramm des menschen," *Archiv für Psychiatrie und Nervenkrankheiten*, vol. 87, no. 1, pp. 527–570, Dec 1929.

[2] G. Buzsáki and A. Draguhn, "Neuronal oscillations in cortical networks," *Science*, vol. 304, no. 5679, pp. 1926–1929, 2004.

[3] X. Wang, "Neurophysiological and computational principles of cortical rhythms in cognition," *Physiological reviews*, vol. 90, no. 3, pp. 1195–1268, 2010.

[4] H. R. Wilson and J. D. Cowan, "Excitatory and inhibitory interactions in localized populations of model neurons," *Biophysical Journal*, vol. 12, no. 1, pp. 1–24, 1972.

[5] B. Baird, "Nonlinear dynamics of pattern formation and pattern recognition in the rabbit olfactory bulb," *Physica D: Nonlinear Phenomena*, vol. 22, no. 1-3, pp. 150–175, 1986.

[6] R. M. Borisyuk and A. B. Kirillov, "Bifurcation analysis of a neural network model," *Biological Cybernetics*, vol. 66, no. 4, pp. 319–325, 1992.

[7] L. H. A. Monteiro, M. A. Bussab, and J. G. C. Berlinck, "Analytical results on a Wilson-Cowan neuronal network modified model," *Journal of Theoretical Biology*, vol. 219, no. 1, pp. 83–91, 2002.

[8] A. C. E. Onslow, M. W. Jones, and R. Bogacz, "A canonical circuit for generating phase-amplitude coupling," *PLOS One*, vol. 9, no. 8, p. e102591, 2014.

[9] S. Campbell and D. Wang, "Synchronization and desynchronization in a network of locally coupled Wilson-Cowan oscillators," *IEEE Transactions on Neural Networks*, vol. 7, no. 3, pp. 541–554, 1996.

[10] K. Morrison, A. Degeratu, V. Itskov, and C. Curto, "Diversity of emergent dynamics in competitive threshold-linear networks: a preliminary report," *arXiv preprint arXiv:1605.04463*, 2016.

[11] E. Nozari and J. Cortés, "Hierarchical selective recruitment in linear-threshold brain networks. Part I: Intra-layer dynamics and selective inhibition," *IEEE Transactions on Automatic Control*, 2018, submitted.

[12] M. Breakspear, S. Heitmann, and A. Daffertshofer, "Generative models of cortical oscillations: neurobiological implications of the Kuramoto model," *Frontiers in human neuroscience*, vol. 4, p. 190, 2010.

[13] L. Tiberi, C. Favaretto, M. Innocenti, D. S. Bassett, and F. Pasqualetti, "Synchronization patterns in networks of Kuramoto oscillators: A geometric approach for analysis and control," in *IEEE Conf. on Decision and Control*, Melbourne, Australia, Dec. 2017, pp. 481–486.

[14] T. Menara, G. Baggio, D. S. Bassett, and F. Pasqualetti, "Stability conditions for cluster synchronization in networks of heterogeneous Kuramoto oscillators," *IEEE Transactions on Control of Network Systems*, 2019, in press.

[15] H. G. Schuster and P. Wagner, "A model for neuronal oscillations in the visual cortex. 1. mean-field theory and derivation of the phase equations," *Biological Cybernetics*, vol. 64, no. 1, pp. 77–82, 1990.

[16] G. B. Ermentrout and N. Kopell, "Oscillator death in systems of coupled neural oscillators," *SIAM Journal on Applied Mathematics*, vol. 50, no. 1, pp. 125–146, 1990.

[17] P. Dayan and L. F. Abbott, *Theoretical Neuroscience: Computational and Mathematical Modeling of Neural Systems*, ser. Computational Neuroscience. Cambridge, MA: MIT Press, 2001.

[18] L. Perko, *Differential Equations and Dynamical Systems*, 3rd ed., ser. Texts in Applied Mathematics. New York: Springer, 2000, vol. 7.

[19] W. Grasman, "Periodic solutions of autonomous differential equations in higher-dimensional spaces," *The Rocky Mountain Journal of Mathematics*, vol. 7, no. 3, pp. 457–466, 1977.

[20] L. A. Sanchez, "Existence of periodic orbits for high-dimensional autonomous systems," *Journal of Mathematical Analysis and Applications*, vol. 363, no. 2, pp. 409–418, 2010.

[21] S. Deneve and C. K. Machens, "Efficient codes and balanced networks," *Nature Neuroscience*, vol. 19, no. 3, p. 375, 2016.

[22] S. F. Muldoon, F. Pasqualetti, S. Gu, M. Cieslak, S. T. Grafton, J. M. Vettel, and D. S. Bassett, "Stimulation-based control of dynamic brain networks," *PLOS Computational Biology*, vol. 12, no. 9, p. e1005076, 2016.

[23] M. Mannino and S. L. Bressler, "Freeman's nonlinear brain dynamics and consciousness," *Journal of Consciousness Studies*, vol. 25, no. 1-2, pp. 64–88, 2018.

[24] I. Ispolatov, V. Madhok, S. Allende, and M. Doebeli, "Chaos in high-dimensional dissipative dynamical systems," *Scientific Reports*, vol. 5, p. 12506, 2015.

[25] H. D. I. Abarbanel, R. Brown, J. J. Sidorowich, and L. S. Tsimring, "The analysis of observed chaotic data in physical systems," *Reviews of Modern Physics*, vol. 65, no. 4, p. 1331, 1993.

[26] H. Haken, "At least one Lyapunov exponent vanishes if the trajectory of an attractor does not contain a fixed point," *Physics Letters A*, vol. 94, no. 2, pp. 71–72, 1983.

[27] P. C. Müller, "Calculation of Lyapunov exponents for dynamic systems with discontinuities," *Chaos, Solitons & Fractals*, vol. 5, no. 9, pp. 1671–1681, 1995.

[28] T. Kreuz, F. Mormann, R. G. Andrzejak, A. Kraskov, K. Lehnertz, and P. Grassberger, "Measuring synchronization in coupled model systems: A comparison of different approaches," *Physica D: Nonlinear Phenomena*, vol. 225, no. 1, pp. 29–42, 2007.

[29] M. L. van Quyen, J. Foucher, J. P. Lachaux, E. Rodriguez, A. Lutz, J. Martinerie, and F. J. Varela, "Comparison of Hilbert transform and wavelet methods for the analysis of neuronal synchrony," *Journal of Neuroscience Methods*, vol. 111, no. 2, pp. 83–98, 2001.

[30] A. B. L. Tort, R. Komorowski, H. Eichenbaum, and N. Kopell, "Measuring phase-amplitude coupling between neuronal oscillations of different frequencies," *Journal of Neurophysiology*, vol. 104, no. 2, pp. 1195–1210, 2010.